Supplementary information

Counting molecules in nano test tubes: a method for determining the activation parameters of thermally driven reactions through direct imaging

Kayleigh L. Y. Fung,[a] Stephen T. Skowron,[a] Christopher S. Allen,[b,c] Andrei N. Khlobystov[a]

[a]School of Chemistry, University of Nottingham, University Park, Nottingham NG7 2RD, UK.

[b]Electron Physical Sciences Imaging Centre, Diamond Light Source Ltd., Oxfordshire OX11 0DE, UK.

[c]Department of Materials, University of Oxford, Parks Road, Oxford OX1 3PH, UK.

Experimental

Reagents were purchased from Sigma Aldrich and used as received.

High resolution transmission electron microscopy (HR-TEM) was carried out at the electron Physical Science Imaging Centre (ePSIC) at Diamond Light Source. The microscope JEOL ARM300F is Cs corrected and was operated at 80 kV. Micrographs were acquired using the Gatan OneView camera. In-situ sample heating with single tilt DENS Solutions Wildfire heating holder, temperature range: ambient to 1200 °C. TEM samples were prepared via a drop casting technique, where samples were dispersed in HPLC-grade isopropanol, followed by deposition of several drops of the suspension onto copper grid mounted with "lacey" carbon films (Agar Scientific UK), and dried under ambient conditions. All micrographs were processed using Gatan Digital Micrograph and ImageJ Fiji software[S1–3] with the ImageJ plugins TurboReg and StackReg.[S4]

Matrix assisted laser desorption/ionisation time-of-flight mass spectrometry (MALDI-ToF MS) analyses were performed on a Bruker ultraFlexIII instrument (Bruker Daltonik, Bremen, Germany). Samples were deposited on a stainless steel target plate (type MTP384; Bruker Daltonik, Bremen, Germany) and due to the nature of the samples, no matrix was required. A pulsed solid-state UV laser (355nm, 500 µJ, 66.7Hz) was used to ionise the sample. The instrument was operated in reflection mode. Data was acquired through the instrument's flexControl software (v3,B185; Bruker Daltonik, Bremen, Germany), and processed using Bruker's flexAnalysis software (v3,B96; Bruker Daltonik, Bremen, Germany).

Nuclear magnetic resonance (NMR) spectroscopy was carried out in deuterated chloroform using a Bruker AV(III)500 spectrometer by Analytical Chemistry at the University of Nottingham. All chemical shifts are quoted in ppm relative to neat trimethylsilate (TMS).

PCC was synthesised as described in literature.[S5,6] ^{13}C NMR δ (500 MHz, $CDCl_3$); 133.2 (Aryl C-Cl), 126.8 (Aryl C), 121.4 (Aryl C). Positive-ion MALDI-ToF MS m/z; 713 ($C_{24}Cl_{12}$), 642 ($C_{24}Cl_{10}$), 571 ($C_{24}Cl_8$), 500 ($C_{24}Cl_6$). See SI section 4 for the spectra.

Single-walled carbon nanotubes (50 mg) were refluxed in nitric acid (3 M, 50 mL) at 120 °C for 2 hr. The nanotubes were then filtered over PTFE membrane (0.2 µm) and washed with sodium hydroxide (1 M, 50 mL) as well as deionised water (50 mL) and dried under vacuum to give dried, opened SWNTs (49.5 mg). Perchlorocoronene was added to the opened nanotubes in a 3:1 mass ratio, sealed in a glass ampoule under vacuum (×10^{-4} mbar) and heated at 400 °C for 72 hr. The resulting black powder was washed by sonicating in toluene and filtering over PTFE membrane (0.2 µm).

Section 1: **Multiple image series of electron beam induced PCC polymerisation at 23 °C**

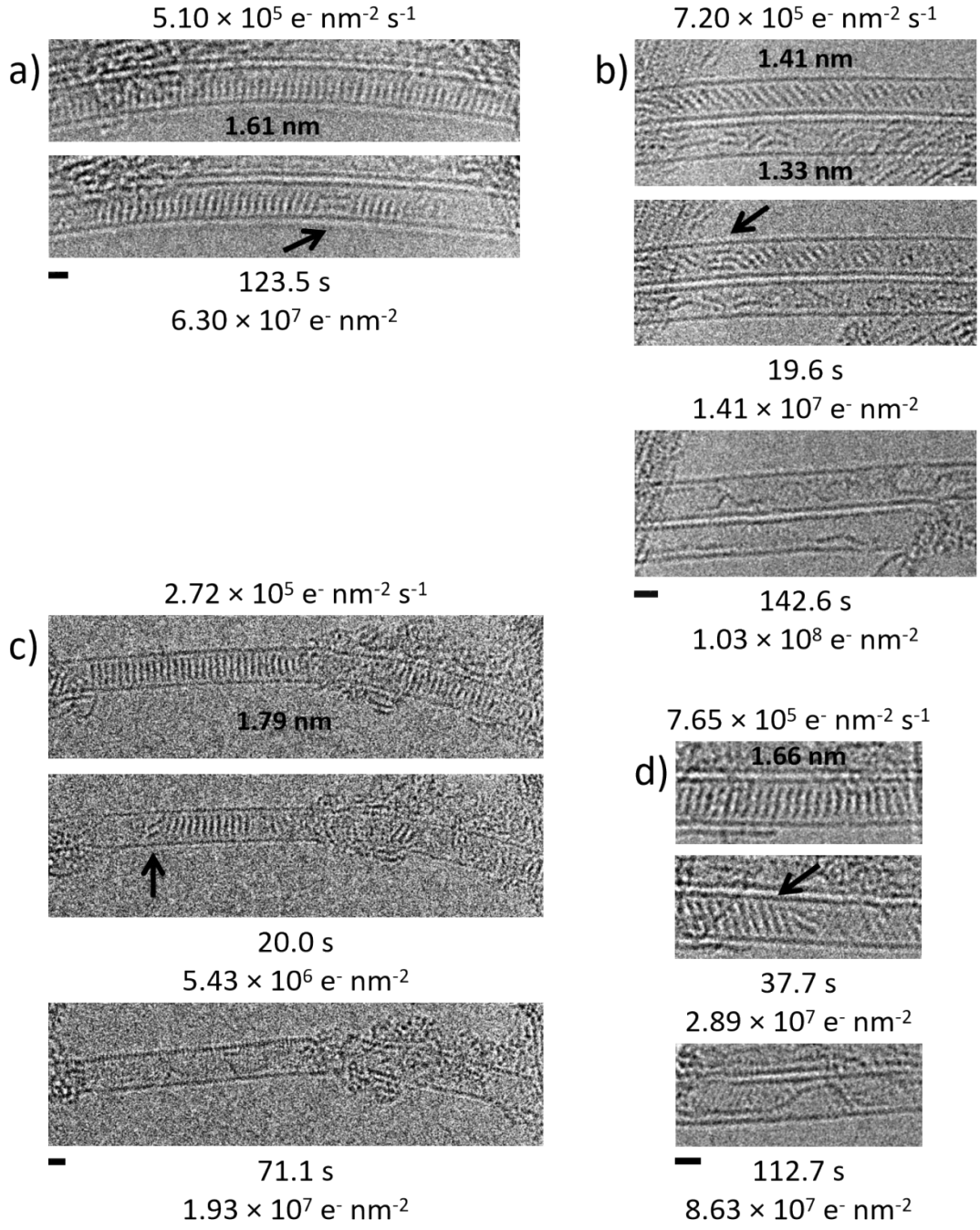

SI Figure 1. Several image series of PCC@SWNT were acquired at 23 °C for comparison to heating experiments. For each series of images, the first image is shown alongside the image of the first dimer (black arrows) and, if present, the final image of the nanoribbon. Electron fluxes, doses, nanotube diameters, and time stamps are shown. All scale bars are 1 nm. Measurements for each nanotube are shown in Table 1 in Section 3.

Section 2: The TEM images acquired after heating cycles at 500, 550, and 600 °C and used for calculating the activation energy

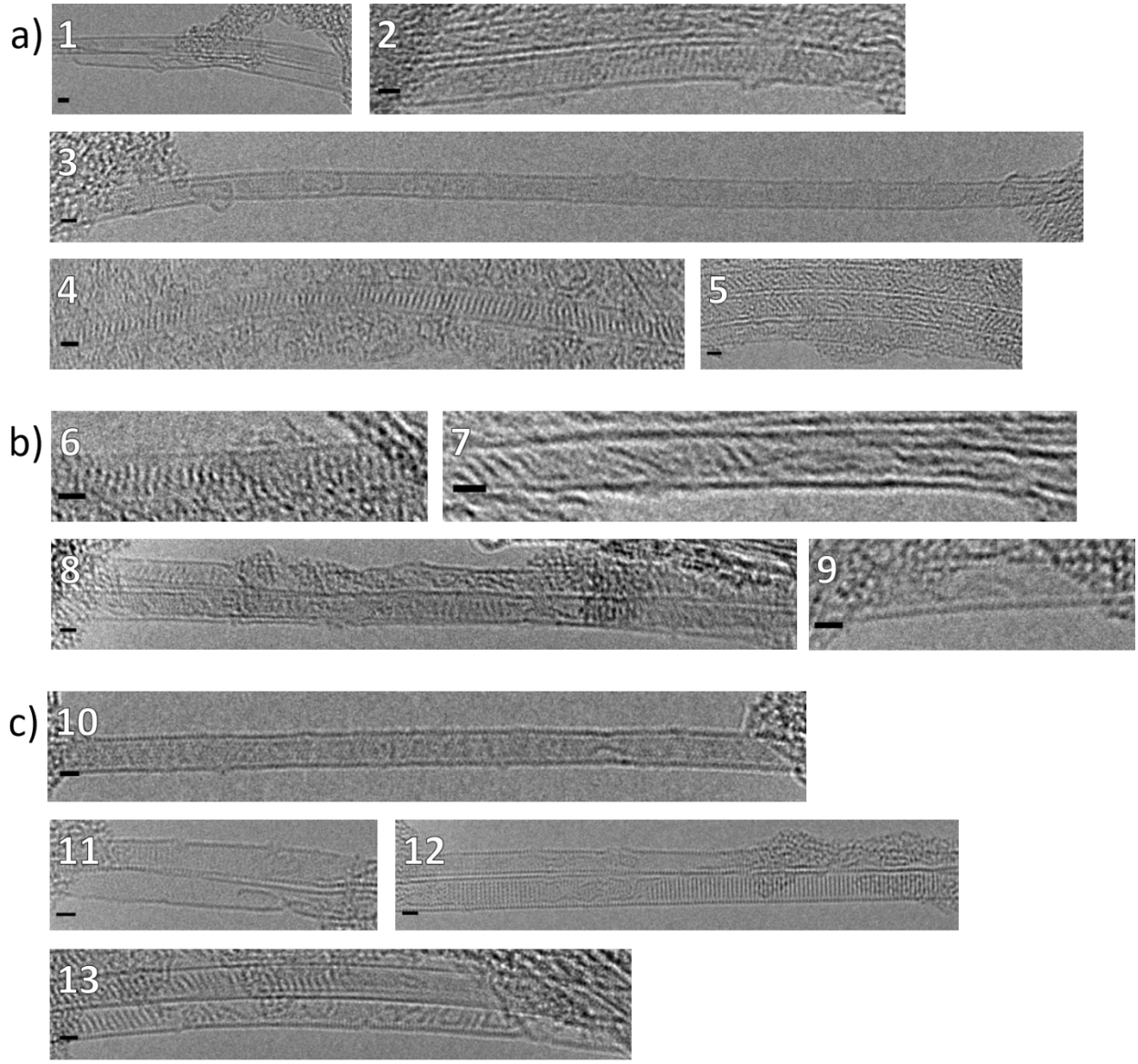

SI Figure 2. PCC@SWNTs heated to 500 °C and held for **a)** 5, **b)** 10, and **c)** 15 minutes. The images were acquired after cooling to ambient temperatures and allowing the sample to equilibrate for 5 minutes. All scale bars are 1 nm. Measurements for each nanotube are shown in Table 1 in Section 3. Nanotube numerical labels correspond to the nanotube IDs in Table 1.

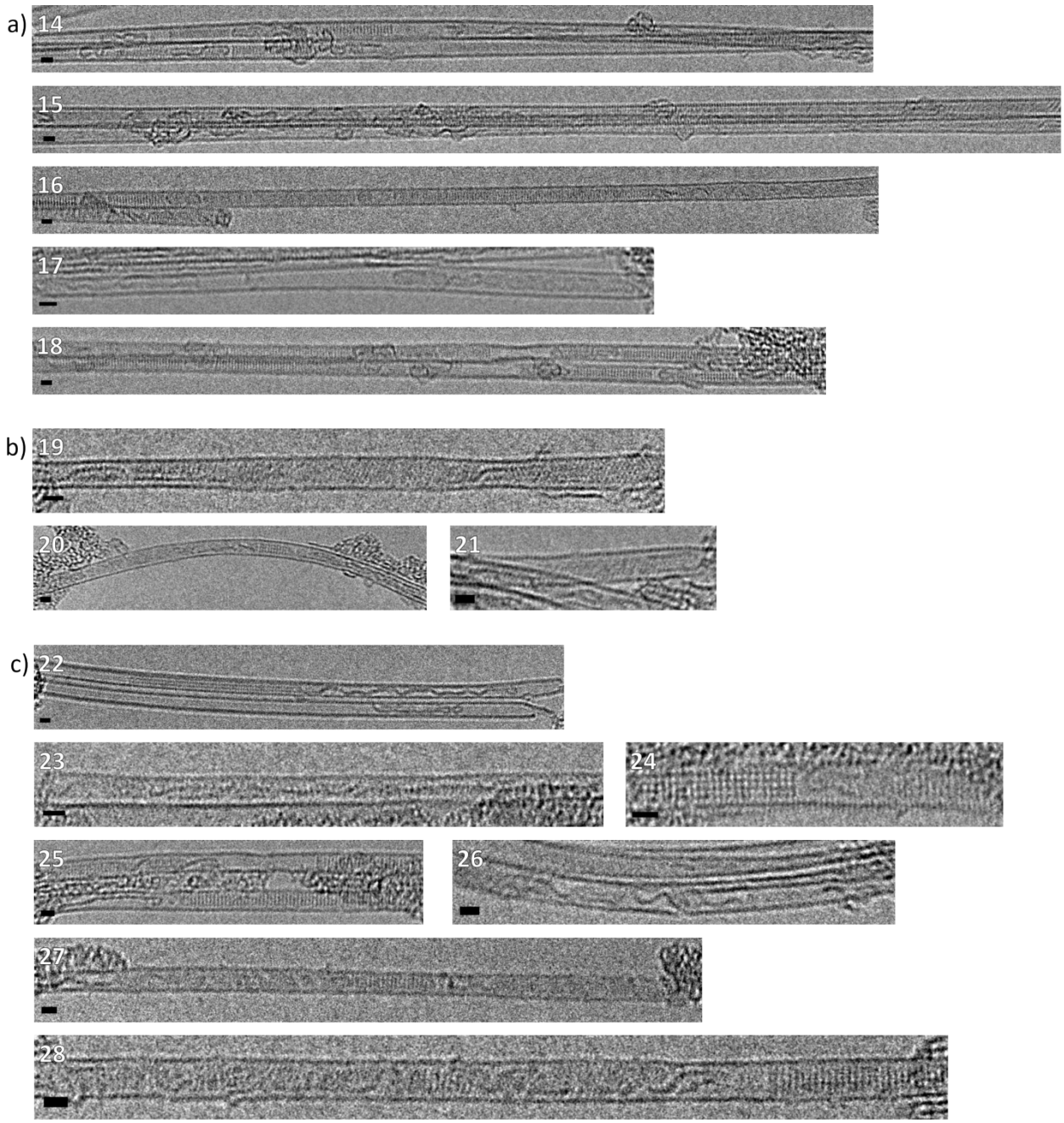

SI Figure 3. PCC@SWNTs heated to 550 °C and held for **a)** 5, **b)** 10, and **c)** 15 minutes. The images were acquired after cooling to ambient temperatures and allowing the sample to equilibrate for 5 minutes. All scale bars are 1 nm. Measurements for each nanotube are shown in Table 1 in Section 3. Nanotube numerical labels correspond to the nanotube IDs in Table 1.

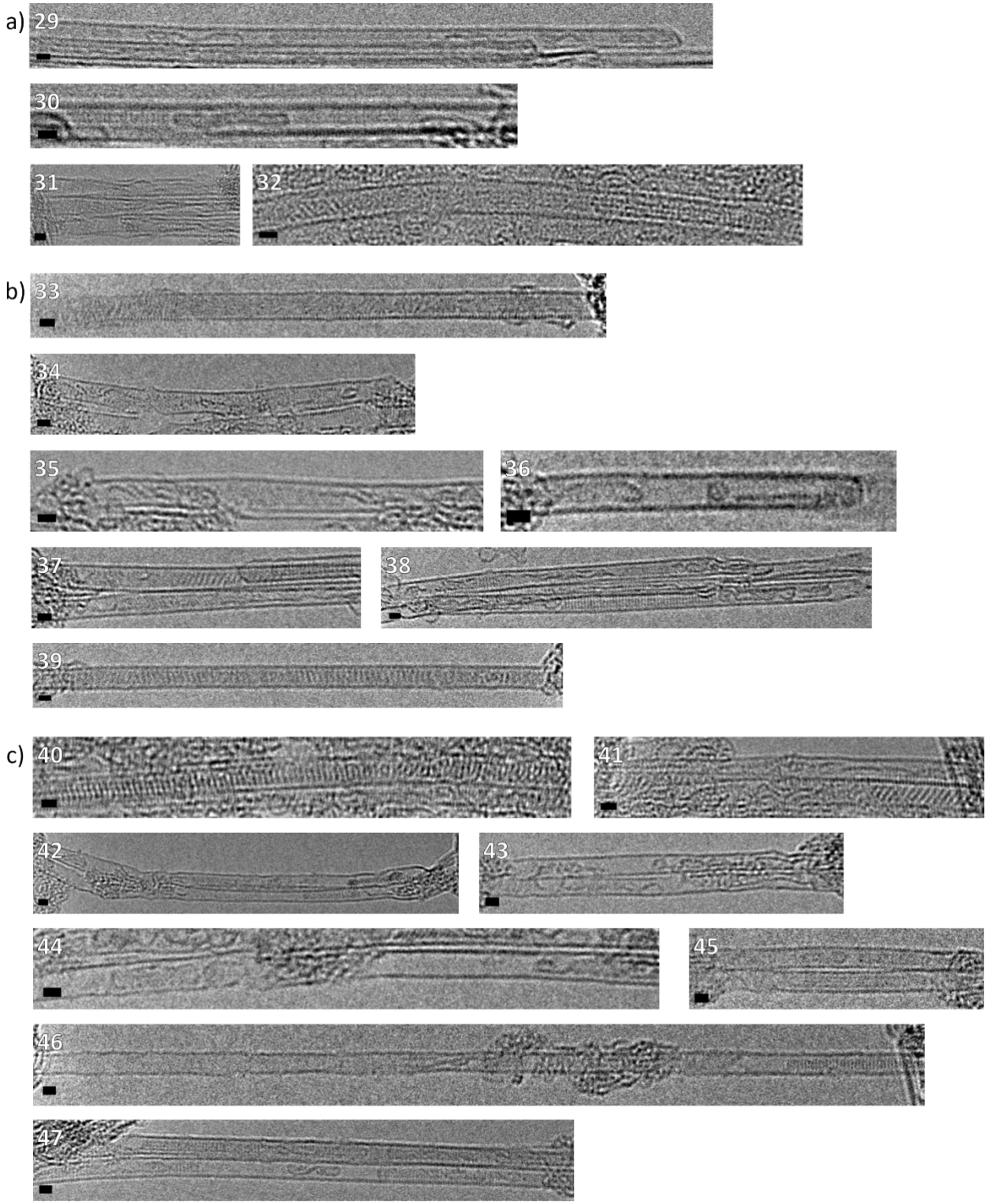

SI Figure 4. PCC@SWNTs heated to 600 °C and held for **a)** 5, **b)** 10, and **c)** 15 minutes. The images were acquired after cooling to ambient temperatures and allowing the sample to equilibrate for 5 minutes. All scale bars are 1 nm. Measurements for each nanotube are shown in Table 1 in Section 3. Nanotube numerical labels correspond to the nanotube IDs in Table 1.

Section 3: Details on the data and calculations for the thermally activated PCC polymerisation

Table 1: Measurements of nanotube volume and number of molecules for each nanotube imaged at 23, 500, 550, and 600 °C.

23 °C (SI Fig. 1)	Number of molecules	Nanotube width in nm	Nanotube length in nm	Nanotube volume in nm^3
a)	57	1.6	21.8	44.5
b) top	25	1.4	11.2	17.5
c)	30	1.8	11.2	28.3
d)	24	1.7	9.0	19.5
500 °C after 5 min (SI Fig. 4a)	Number of molecules	Nanotube width in nm	Nanotube length in nm	Nanotube volume in nm^3
1 top	0	1.8	26.3	66.6
2	31	1.6	21.3	41.0
3	0	1.5	58.5	103.8
4	80	1.5	32.8	60.6
5 top	24	1.4	22.1	32.9
5 middle	5	1.4	20.8	32.9
500 °C after 10 min (SI Fig. 4b)	Number of molecules	Nanotube width in nm	Nanotube length in nm	Nanotube volume in nm^3
6	29	1.6	10.3	21.7
7	4	1.5	16.7	29.8
8 top	13	1.5	38.3	68.4
8 bottom	9	1.6	39.8	75.3
9	0	1.5	9.9	17.1

500 °C after 15 min (SI Fig. 4c)	Number of molecules	Nanotube width in nm	Nanotube length in nm	Nanotube volume in nm^3
10	0	1.6	36.6	74.2
11 top	0	1.7	11.8	26.3
12 top	0	1.2	21.2	25.5
12 bottom	85	1.9	33.5	91.6
13 top	33	1.7	22.4	50.2
13 bottom	10	1.9	24.4	68.0
550 °C after 5 min (SI Fig. 5a)	Number of molecules	Nanotube width in nm	Nanotube length in nm	Nanotube volume in nm^3
14 top	19	1.3	61.1	75.5
14 bottom	0	1.4	61.6	89.2
15 top	2	1.6	85.0	159.3
15 bottom	0	1.4	85.3	135.0
16	28	1.3	76.3	107.1
17	0	1.3	33.5	47.0
18 top	23	1.8	63.5	168.8
18 bottom	38	1.7	63.8	143.8
550 °C after 10 min (SI Fig. 5b)	Number of molecules	Nanotube width in nm	Nanotube length in nm	Nanotube volume in nm^3
19	0	1.3	27.2	33.7
20	10	1.4	21.1	32.7
21	0	1.4	11.0	17.0

550 °C after 15 min (SI Fig. 5c)	Number of molecules	Nanotube width in nm	Nanotube length in nm	Nanotube volume in nm^3
22 top	0	1.3	49.3	67.4
22 bottom	0	1.2	46.3	55.4
23	0	1.2	19.7	23.5
24	20	1.5	12.5	22.3
25 top	20	1.3	26.8	36.5
25 bottom	54	1.3	24.4	34.2
26 bottom	0	1.4	19.7	28.6
27	12	1.3	38.3	50.5
28	29	1.5	34.7	62.1
600 °C after 5 min (SI Fig. 6a)	Number of molecules	Nanotube width in nm	Nanotube length in nm	Nanotube volume in nm^3
29	0	1.2	45.9	52.8
30	0	1.4	21.5	32.2
31 top	0	1.3	15.6	21.1
31 middle	0	1.4	14.6	22.8
31 bottom	0	1.4	12.3	18.4
32	8	1.5	25.9	46.2

600 °C after 10 min (SI Fig. 6b)	Number of molecules	Nanotube width in nm	Nanotube length in nm	Nanotube volume in nm^3
33	0	1.6	25.9	49.6
34	0	1.6	24.8	50.1
35	0	1.5	20.4	36.2
36	0	1.3	12.9	17.3
37 top	11	1.6	12.3	24.2
37 bottom	0	1.4	19.9	29.7
38 top	6	1.5	26.5	46.0
38 bottom	47	1.6	33.6	63.3
39	35	1.5	36.1	64.1
600 °C after 15 min (SI Fig. 6c)	Number of molecules	Nanotube width in nm	Nanotube length in nm	Nanotube volume in nm^3
40	86	1.8	32.1	77.6
41 top	0	1.3	12.6	15.4
41 bottom	11	1.5	8.0	14.1
42 top	0	1.5	25.0	41.8
42 bottom	0	1.5	21.5	38.2
43 top	0	1.3	20.4	26.0
43 bottom	0	1.1	20.9	20.1
44	0	1.4	32.3	48.3
45 top	0	1.3	16.3	21.4
45 bottom	0	1.3	15.3	20.8
46	31	1.5	62.5	110.8
47 top	0	1.2	32.2	37.1
47 bottom	0	1.3	35.5	48.2

Table 2: The measurements in **Table 1** were used for the calculation of the average number of molecules per volume of nanotube, or nPCC/V.

Temperature in Celsius	Temperature in Kelvin	Time in s	Total number of PCC molecules	Total nanotube volume (V) in nm^3	Average nPCC/V in nm^{-3}
23.00	296.15	N/A	136	109.7	1.25
500.00	773.15	304.66	140	337.8	0.41
500.00	773.15	639.59	55	212.4	0.26
500.00	773.15	946.90	128	335.8	0.38
550.00	823.15	302.01	110	925.7	0.12
550.00	823.15	605.35	10	83.37	0.12
550.00	823.15	926.34	135	380.5	0.36
600.00	873.15	301.76	8	193.5	0.04
600.00	873.15	603.88	99	380.4	0.26
600.00	873.15	913.56	128	519.7	0.25

Table 3: The values in **Table 2** were used to calculate k_T.

Experiment	k_T in $nm^3\ s^{-1}$
500 for 5 min	0.0053
500 for 10 min	0.0048
500 for 15 min	0.0019
550 for 5 min	0.0252
550 for 10 min	0.0124
550 for 15 min	0.0022
600 for 5 min	0.077
600 for 10 min	0.0050
600 for 15 min	0.0036

Table 4: The values in **Table 3** were averaged for each temperature used and $\ln(k_T/T)$ was plotted against 1/T (see main text). The standard deviations of each average value were used as the error bars.

Average $\ln(k_T/T)$ in $nm^3\ s^{-1}\ K^{-1}$	Standard deviation of $\ln(k_T/T)$	1/T in K^{-1}
-12.17	0.56	0.0013
-11.04	1.26	0.0012
-10.32	1.69	0.0011

Table 5: The plot of $\ln(k_T/T)$ against 1/T was used to find enthalpy of activation ($\Delta H^{\ddagger}$), entropy of activation ($\Delta S^{\ddagger}$), as well as the free energy of activation ($\Delta G^{\ddagger}$).

$\Delta H^{\ddagger}$ (kJ mol^{-1})		104.3
$\Delta H^{\ddagger}$ (eV mol^{-1})		1.081
$\Delta S^{\ddagger}$ (kJ $mol^{-1}\ K^{-1}$)		-0.163
$\Delta S^{\ddagger}$ (eV $mol^{-1}\ K^{-1}$)		-0.0017
$\Delta S^{\ddagger}$ (cal $mol^{-1}\ K^{-1}$)		-39.08
	T (K)	$\Delta G^{\ddagger}$
$\Delta G^{\ddagger}$ (kJ mol^{-1})	773.15	230.7
	823.15	238.9
	873.15	247.0
$\Delta G^{\ddagger}$ (eV mol^{-1})	773.15	2.391
	823.15	2.476
	873.15	2.560

Table 6: Calculation of the standard deviation in enthalpy of activation ($\Delta H^{\ddagger}$), entropy of activation ($\Delta S^{\ddagger}$), and the free energy of activation ($\Delta G^{\ddagger}$).

$\sigma\Delta H/k_B{}^{\ddagger}$ (the gradient in s^{-1})		1224.8
$\sigma\Delta H$ (kJ mol^{-1})		10.18
$\sigma\Delta H$ (eV mol^{-1})		0.106
$\sigma\ln(k_B/h)+\Delta S/k_B$ (y-intercept)		1.493
$\sigma\Delta S^{\ddagger}$ (kJ mol^{-1} K^{-1})		-0.185
$\sigma\Delta S^{\ddagger}$ (eV mol^{-1} K^{-1})		-0.002
$\sigma\Delta S^{\ddagger}$ (cal mol^{-1} K^{-1})		-44.25
	T (K)	$\sigma\Delta G^{\ddagger}$
$\sigma\Delta G^{\ddagger}$ (kJ mol^{-1})*	773.15	143.5
	823.15	152.7
	873.15	162.0
$\sigma\Delta G^{\ddagger}$ (eV mol^{-1})*	773.15	1.487
	823.15	1.583
	873.15	1.679

*Calculation of standard deviation using error propagation:

$$\sigma\Delta G^{\ddagger} = \sqrt{\sigma\Delta H^{\ddagger 2} + (T.\sigma\Delta S^{\ddagger})^2}$$

Section 4: Application of the Arrhenius equation to our data and estimation of the entropic effect of encapsulation of PCC molecules into single-walled carbon nanotubes.

The Arrhenius equation:

$$k_T = A \times e^{-\frac{E_a}{k_B T}}$$

links *kT* values with the activation energy of thermally driven polymerisation, *Ea*. *T* is the temperature, *A* is the pre-exponential factor, and k_B is the Boltzmann constant (8.617×10^{-5} eV K^{-1}).

Plotting the experimental data as $ln(k_T)$ against *1/T* shows a clear thermal dependence of *kT*. The activation energy was calculated to be 0.658 eV per molecule (63.5 kJ mol^{-1}), with a significant source of uncertainly related to the asymmetrical distributions of *nPCC/V* where high numbers of unreacted PCC molecules occur with very low frequencies, but still contribute to the calculation of *Ea* (see SI Fig. 5).

$$ln(k_T) = -\frac{E_a}{k_B}\left(\frac{1}{T}\right) + ln(A)$$

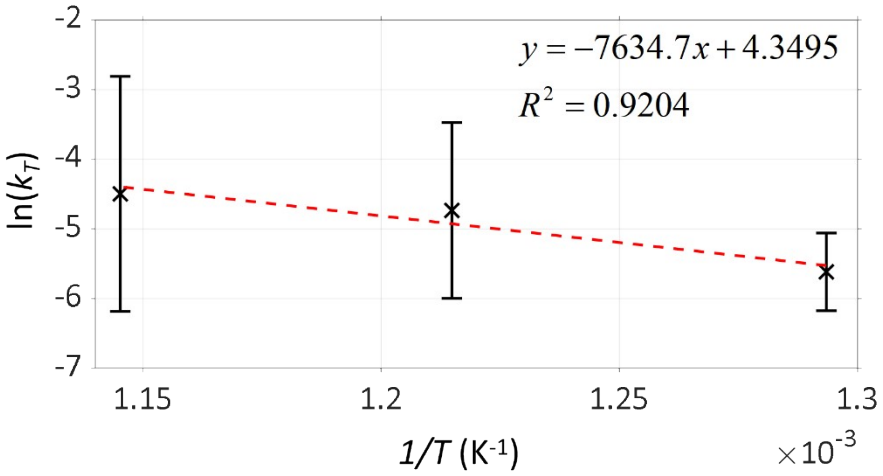

SI Figure 4. The activation energy *Ea* can be calculated for the thermally induced polymerisation of PCC using a linear plot of $ln(k_T)$ against *1/T*.

The Q-Chem 5.0 quantum chemistry software package[S7] was used to perform a geometry optimisation and vibrational analysis of a molecule of PCC (shown in Fig. 1 of the main text), using the ωB97X-D exchange-correlation functional[S8] and 6-311G* basis set. The entropic contributions at standard temperature and pressure were calculated as:

Translational entropy S_t = 0.19059 kJ $^{-1}$ mol $^{-1}$ K $^{-1}$ (45.551 cal mol^{-1} K^{-1})

Rotational entropy S_r = 0.16245 kJ $^{-1}$ mol $^{-1}$ K $^{-1}$ (38.826 cal mol^{-1} K^{-1})

Vibrational entropy S_v = 0.45355 kJ $^{-1}$ mol $^{-1}$ K $^{-1}$ (108.398 cal mol^{-1} K^{-1})

To give the total entropy for a molecule of PCC in the gas phase **S_{tot} (gas) = 0.808 kJ $^{-1}$ mol $^{-1}$ K $^{-1}$ (193 cal mol^{-1} K^{-1})**.

As the three reaction temperatures used experimentally (500, 550, 600 °C) were all approximately at or above the bulk crystal melting point (T_m = 499-561 °C[S6]), we can consider the equivalent bulk reaction as occurring in the liquid (molten) phase. The total entropy in the liquid phase can be calculated by subtracting the entropy of vaporisation ΔS_{vap} - estimated using Trouton's rule[S9] $\Delta S_{vap}(T_B) = \Delta H_{vap}(T_B)/T_B \approx 10.5R \approx 0.088$ kJ $^{-1}$ mol $^{-1}$ K $^{-1}$ (21 cal mol^{-1} K^{-1}) (where T_B is the boiling point and R is the ideal gas constant) - from the total gas-phase entropy to give **S_{tot} (liquid) = 0.720 kJ $^{-1}$ mol $^{-1}$ K $^{-1}$ (172 cal mol^{-1} K^{-1})**.

In the one-dimensional nanoconfined molecular crystal 'stacks', each molecule will possess approximately the same number of vibrational degrees of freedom as in the gas phase, while being limited to only one rotational degree of freedom and zero translational degrees of freedom. The total entropy can therefore be estimated as **S_{tot} (confined) = $S_v + S_r/3$ = 0.506 kJ $^{-1}$ mol $^{-1}$ K $^{-1}$ (121 cal mol^{-1} K^{-1})**.

The total change in entropy of a reactant PCC molecule upon confinement in the carbon nanotube is therefore approximately **ΔS_{encaps} = 0.21 kJ $^{-1}$ mol $^{-1}$ K $^{-1}$ (50 cal mol^{-1} K^{-1})**, and encapsulation represents a 25-30% change in the entropic contribution to the molecular energy, compared to molecules in the gas or liquid phase respectively. At the reaction temperatures used, this equates to a **105-127 kJ mol^{-1} (1.1-1.3 eV)** increase in the molecular reactant free energy.

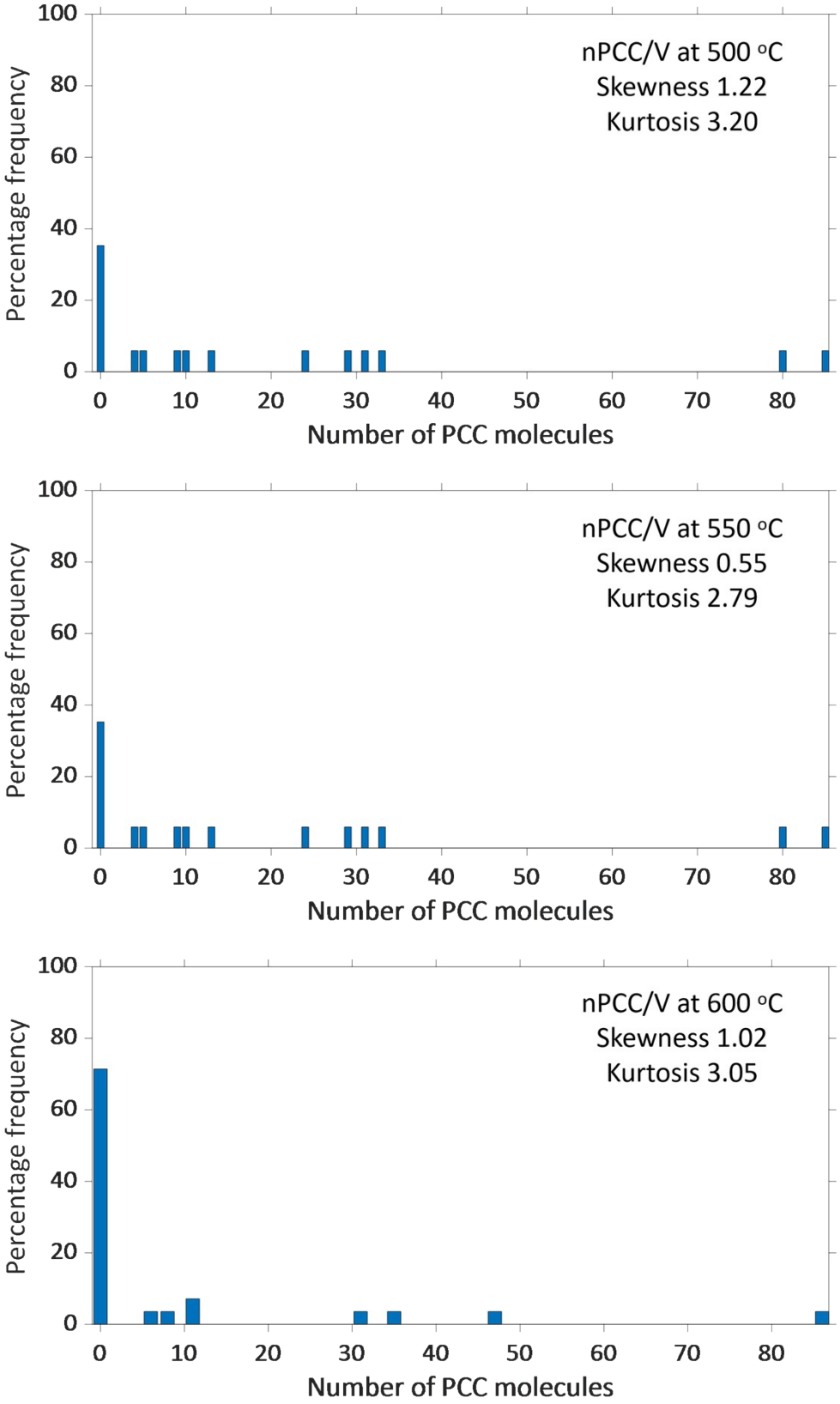

SI Figure 5. The asymmetrical distributions of the number of PCC molecules (nPCC) across the three elevated temperatures (500, 550, and 600 °C). A normal distribution will have a kurtosis of 3. Values of kurtosis above 3 indicate that the distribution is leptokurtic, or produces more outliers than the normal distribution. A normal distribution will have a skewness of 0. All three data sets have a positive skew, meaning that the data are asymmetric and spreads out more to the right.

Section 5: Characterisation of PCC

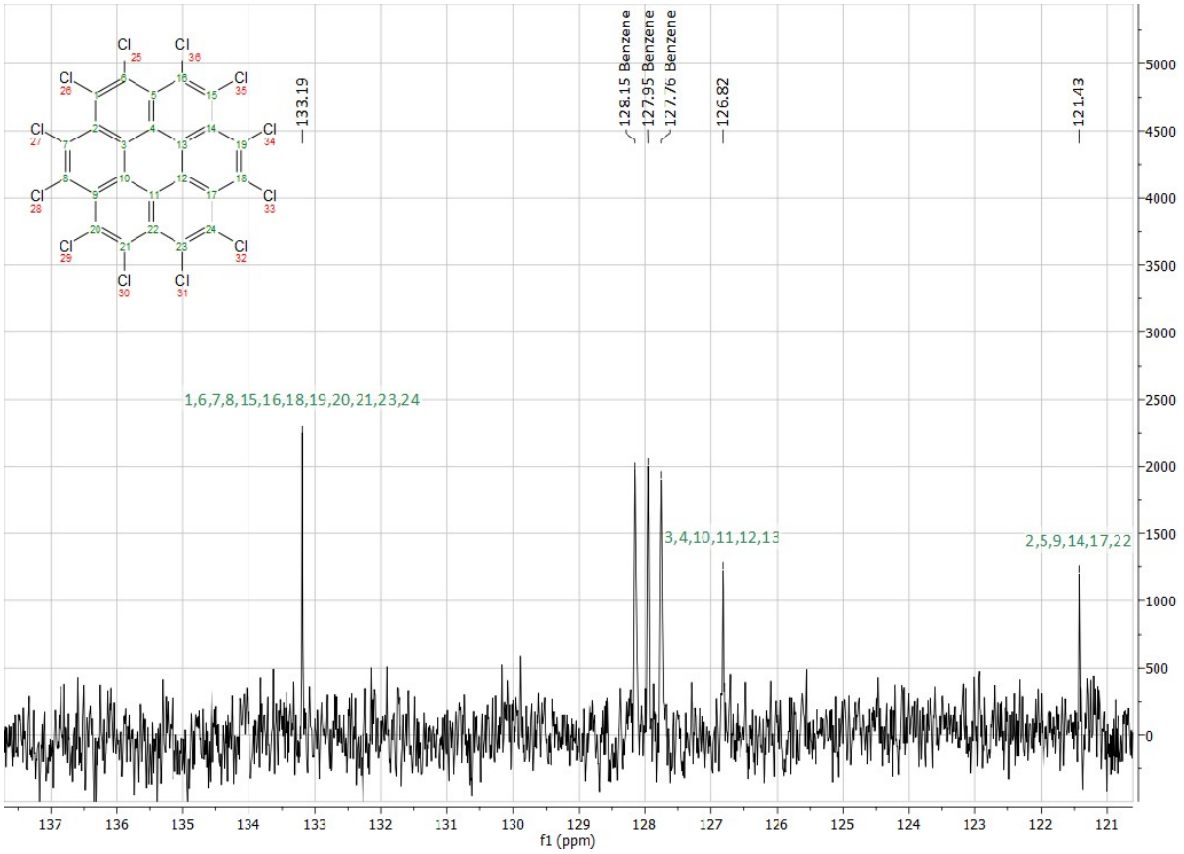

SI Figure 6. The ^{13}C NMR spectrum of PCC. The PCC peaks are labelled with the structure adjacent.

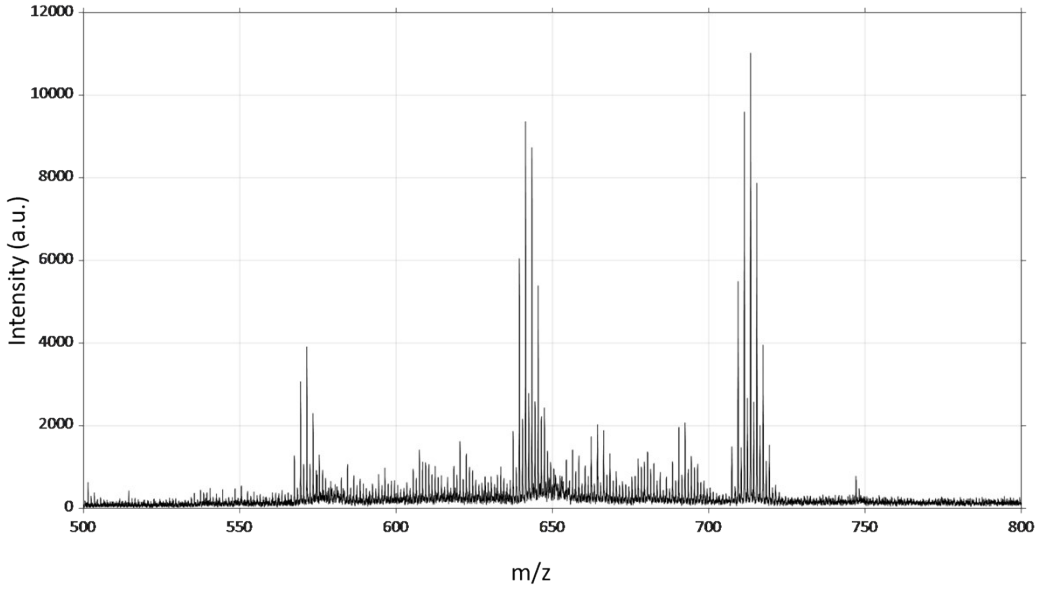

SI Figure 7. The MALDI-ToF spectrum of PCC. No matrix was used.

References

S1. Schneider, C. A., Rasband, W. S. & Eliceiri, K. W. NIH Image to ImageJ: 25 years of image analysis. *Nat. Methods* **9**, 671–675 (2012).

S2. Schindelin, J. *et al.* Fiji: an open-source platform for biological-image analysis. *Nat. Methods* **9**, 676–682 (2012).

S3. Schindelin, J., Rueden, C. T., Hiner, M. C. & Eliceiri, K. W. The ImageJ ecosystem: An open platform for biomedical image analysis. *Mol. Reprod. Dev.* **82**, 518–529 (2015).

S4. Thevenaz, P., Ruttimann, U. E. & Unser, M. A pyramid approach to subpixel registration based on intensity. *IEEE Trans. Image Process.* **7**, 27–41 (1998).

S5. Ballester, M., Molinet, C. & Castaner, J. Preparation of Highly Strained Aromatic Chlorocarbons. I. A Powerful Nuclear Chlorinating Agent. Relevant Reactivity Phenomena Traceable to Molecular Strain. *J Am Chem Soc* **82**, 4254–4258 (1960).

S6. Koshino, M., Kurata, H. & Isoda, S. Study of structures at the boundary and defects in organic thin films of perchlorocoronene by high-resolution and analytical transmission electron microscopy. *Ultramicroscopy* **110**, 1465–1474 (2010).

S7. Epifanovsky, E. *et al.* Software for the frontiers of quantum chemistry: An overview of developments in the Q-Chem 5 package. *J. Chem. Phys.* **155**, 084801 (2021).

S8. Chai, J.-D. & Head-Gordon, M. Long-range corrected hybrid density functionals with damped atom–atom dispersion corrections. *Phys. Chem. Chem. Phys.* **10**, 6615–6620 (2008).

S9. Trouton, F. IV. On molecular latent heat. *Lond. Edinb. Dublin Philos. Mag. J. Sci.* **18**, 54–57 (1884).